JOURNAL OF SOLID STATE CHEMISTRY 105, 287–293 (1993)

The Structure and Properties of an Unusual New Nickel(III) Oxide: $YSr_5Ni_3O_{11}$

M. JAMES* AND J. P. ATTFIELD

Department of Chemistry, University of Cambridge, Lensfield Road, Cambridge, CB2 1EW, United Kingdom; and Interdisciplinary Research Centre in Superconductivity, University of Cambridge, Madingley Road, Cambridge, CB3 OHE, United Kingdom

Received August 17, 1992; in revised form November 10, 1992; accepted November 11, 1992

An investigation of the system $Y_{2-x}Sr_xNiO_{4-\delta}$ has shown that a stable phase exists only at $x = 1.67$ between 1100 and 1150°C. Thermogravimetric analysis gives the oxygen deficiency as $\delta = 0.33(1)$, showing that the phase is a stoichiometric nickel(III) oxide, $YSr_5Ni_3O_{11}$ ($Y_{0.33}Sr_{1.67}NiO_{3.67}$). Rietveld refinement using powder X-ray diffraction data confirms that $YSr_5Ni_3O_{11}$ adopts the tetragonal K_2NiF_4 (T-type) structure (*I4/mmm*, $Z = \frac{2}{3}$, $a = 3.7762(1)$, $c = 12.3011(4)$ Å, $R_{wp} = 3.9\%$). Independent refinement of the oxygen site occupancies reveals that the oxygen vacancies are present in the nickel oxide planes. Magnetic susceptibility data for $YSr_5Ni_3O_{11}$ at 5–350 K show Curie–Weiss behavior characteristic of low spin Ni^{3+} with $\mu_{eff} = 1.76$ and $\Theta = -10.8$ K. Four-probe dc electronic conductivity measurements show that the material is a semiconductor between 7 and 300 K. These data are well fitted by a two-dimensional variable range hopping model.

Introduction

Many mixed oxides of the type A_2BO_4 (A = rare earth, B = transition metal) crystallize with the tetragonal K_2NiF_4 (T-type) structure (Fig. 1) in space group *I4/mmm*. They are composed of alternating perovskite (ABO_3) and rock-salt (AO) layers along the tetragonal c axis. This places the larger A^{3+} ions in ninefold coordination, forming double layers between octahedrally coordinated B^{2+} ions. BO_6 octahedra share corners in the ab plane, forming a two-dimensional array of B–O–B bonds which give these compounds quasi-two-dimensional magnetic and electrical properties (*1–4*).

Following the discovery of superconductivity in the $La_{2-x}Sr_xCuO_4$ system (*5*), many authors have reported studies on nickel oxides having the same structure. In particular, extensive investigations have been carried out on the structural, magnetic, and electrical properties of the $La_{2-x}Sr_xNiO_{4-\delta}$ (*6–8*) and $Nd_{2-x}Sr_xNiO_{4-\delta}$ (*9, 10*) solid solutions. Despite claims for the onset of diamagnetism and superconductivity in the $La_{2-x}Sr_xNiO_{4-\delta}$ system (*11–14*), no pure superconducting nickel oxide phase has yet been isolated. As a part of a study of $R_{2-x}Sr_xNiO_{4-\delta}$ phases with smaller R^{3+} cations we present an investigation of the R = Y system. No phases for $0 \leq x \leq 2$ have previously been reported.

Experimental

Sample Preparation

Polycrystalline samples with bulk composition $Y_{2-x}Sr_xNiO_{4-\delta}$ ($1.0 \leq x \leq 1.8$) were synthesized from spectroscopic grade powders of strontium carbonate, nickel nitrate hexahydrate, and yttrium oxide. Prior to weighing, the Y_2O_3 was preheated to 1000°C in air to decompose any carbonate material from the oxide. The powders were dissolved

*To whom correspondence should be addressed.

0022-4596/93 $5.00

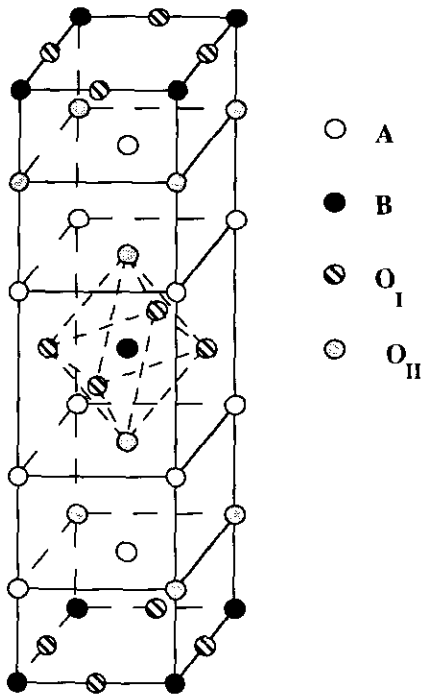

FIG. 1. Crystal structure of A_2BO_4 with the tetragonal K_2NiF_4 structure type.

in dilute nitric acid, and an intimate mixture of the metal oxides was formed via the decomposition of a citric acid/ethylene glycol gel. The residues were pelleted and sintered in a tube furnace under flowing oxygen. Samples were repelleted and reheated until no further reaction was evident by powder X-ray diffraction.

Thermogravimetric Analysis

Thermogravimetric analysis (TGA) of a freshly annealed sample of approximately 15 mg was carried out using a Stanton Redcroft STA 1500 simultaneous thermal analyzer. The sample was reduced under a 5% hydrogen in nitrogen mixture (flow rate of 48 ml/min), over a temperature range of 50–950°C at a heating rate of 5°C per minute.

Powder X-Ray Diffraction (XRD)

Powder X-ray diffraction profiles were recorded on a Phillips PW1710 diffractometer, utilizing Cu$K\alpha$ radiation. Indexed peak positions were used to refine the cell parameters. Data of sufficient quality for structural refinement were collected over $13 \leq 2\Theta \leq 103°$, in 0.025° steps, with integration times of 15 sec. The Rietveld refinement (*15*) was performed with the GSAS program (*16*), using a refined background function.

Magnetic Susceptibility Measurements

Variable temperature measurements of magnetic susceptibility were conducted using a Quantum Design SQUID magnetometer. Measurements were made under an applied field of 3.0 T. Samples were cooled to 5 K in zero field prior to measurement of the magnetization. The temperature was then raised in increments of either 2.5 or 5 K until an upper limit of 350 K was reached.

Conductivity Measurements

Conductivity measurements were carried out in a liquid helium cooled Oxford Instruments flow cryostat, using the conventional four-probe dc technique. The sample was pressed into a 13 mm diameter pellet, sintered at 1200°C overnight, and slowly cooled in flowing oxygen. A bar of approximate dimensions 1 × 5 × 8 mm was cut from the pellet and mounted onto the probe with double-sided adhesive tape, and copper wires were attached using colloidal silver paint. The sample was cooled at 5°C/min and the temperature was measured using a calibrated silicon diode thermometer, mounted about 5 mm from the sample on a copper block.

Results

Initial attempts to prepare "$YSrNiO_4$" resulted in a mixture of phases including a Sr-rich K_2NiF_4 type component at temperatures above 1100°C. The compositions $Y_{2-x}Sr_xNiO_{4-\delta}$ ($1.0 \leq x \leq 1.8$) were subsequently investigated at this temperature. For $x < 1.67$, mixtures of Y_2SrO_4, NiO, and the new K_2NiF_4 type phase were found,

TABLE I

OBSERVED *d*-SPACINGS AND INTENSITIES OF PEAKS FROM THE POWDER X-RAY DIFFRACTION PATTERN OF $YSr_5Ni_3O_{11}$

(*hkl*)	*d*-Spacing (Å)	Relative Intensity
002	6.141	7
101	3.610	8
004	3.075	8
103	2.778	100
110	2.670	82
112	2.449	2
105	2.061	14
006	2.050	12
114	2.016	24
200	1.888	37
202	1.804	1
211	1.673	2
116	1.626	10
204	1.609	5
107	1.593	4
213	1.562	30
008	1.538	3
215	1.392	9
206	1.389	10
220/118	1.335	9

while compositions with $x > 1.67$ produced SrO, NiO, and the new phase. A pure sample was obtained only for $x = 1.67$ at 1100°C and was found to be stable up to 1150°C in air-quenched products. A sample of $Y_{0.33}Sr_{1.67}NiO_{4-\delta}$, slow-cooled from 1100°C under flowing O_2 to maximize the oxygen content, was used for further characterization.

The oxygen content of $Y_{0.33}Sr_{1.67}NiO_{4-\delta}$ was determined by thermogravimetric analysis. A weight loss of 8.2(2)% was observed between 50 and 950°C due to the reduction of nickel, corresponding to $\delta = 0.33(1)$. This demonstrates that this new phase is a stoichiometric nickel(III) compound $YSr_5Ni_3O_{11}$ ($Y_{0.33}Sr_{1.67}NiO_{3.67}$).

The powder X-ray diffraction pattern of $YSr_5Ni_3O_{11}$ (Table I) was indexed upon a tetragonal K_2NiF_4 type cell with $a = 3.7763(7)$ and $c = 12.303(3)$ Å. A Rietveld refinement of the structure was carried out using data from the long powder X-ray diffraction scan in space group *I4/mmm*, with Y and Sr randomly distributed over the K sites. A good fit was obtained using a pseudo-Voigt peak shape function and the peak width variation was found to be instrument limited. In the final stages, the Sr/Y atom was refined anisotropically while the isotropic temperature factors for O(1) and O(2) were constrained to be equal and their site occupancies were refined independently. Results of the refinement are given in Table II and interatomic distances are listed in Table III. The observed, calculated, and difference profiles are displayed in Fig. 2.

The molar susceptibility (χ_M) of $YSr_5Ni_3O_{11}$ is shown in Fig. 3. These data were fitted by the equation $\chi_M = \chi_0 + C_M \cdot (T - \Theta)^{-1}$, where the term χ_0 allows for a Van Vleck component, giving the values (per Ni^{3+} ion); $\chi_0 = 0.0023(1)$ emu mole^{-1}, $\mu_{eff} = 1.76(1)$, and $\Theta = -10.8(1)$ K. $(\chi_M - \chi_0)^{-1}$ was found to vary linearly with T over the entire temperature range, as is also shown in Fig. 3.

The electrical conductivity (σ) measurements of $YSr_5Ni_3O_{11}$ show that it is a semiconductor between 5 and 300 K with a 300 K conductivity of 17 $\Omega^{-1}cm^{-1}$. The data have been fitted using equations $\sigma = \sigma_0 \exp(-(E_H/kT)^n)$ which can describe a simple semiconducting model ($n = 1$) and two ($n = \frac{1}{3}$) and three ($n = \frac{1}{4}$) dimensional variable range hopping models (*17*). Figure 4 shows the plots of $\ln(\sigma)$ versus T^{-n}. The two variable range hopping models give a good fit to the data, with the two dimensional model giving a slightly better fit at low temperatures. The characteristic energy for electron hopping between sites in this model is $E_H = 0.012$ eV.

Discussion

Neither the end members Y_2NiO_4 and $Sr_2NiO_{4-\delta}$ nor any solid solutions between them have been reported. The calculated tolerance factor (*18*) for Y_2NiO_4 using Shannon's ionic radii (*19*) is $t = 0.837$, which is below the limit of 0.85 above which stable

TABLE II

PROFILE AND STRUCTURAL PARAMETERS FROM THE REFINEMENT OF $YSr_5Ni_3O_{11}$ IN SPACE GROUP *I4/mmm*, WITH ESD'S IN PARENTHESES

Cell dimensions (Å)

$a = 3.7762(1)$ $c = 12.3011(4)$

Data

No. of reflections = 44 No. of points = 3600 No. of parameters = 21

R factors (%)

$R_{WP} = 3.9$ $R_P = 2.5$ $R_F = 5.6$

Atomic parameters

Atom	Symmetry position	*x*	*y*	*z*	$100 \times U_{iso}$, Å^2	Site occupancy
Ni	2*a*	0	0	0	1.0(1)	1.0
Sr	4*e*	0	0	0.3577(1)	0.9(1)[a]	0.833
Y	4*e*	0	0	0.3577	0.9	0.167
O(1)	4*c*	0.5	0	0	1.4(3)	0.86(1)
O(2)	4*e*	0	0	0.1621(5)	1.4	0.98(1)

[a] Equivalent U_{iso} for Sr/Y, refined anisotropic values ($\times 100$) were U_{11} ($=U_{22}$) = 0.6(1), U_{33} = 1.3(1) Å^2.

K_2NiF_4 type phases may exist. No $Sr_2NiO_{4-\delta}$ materials have been prepared, as near-stoichiometric phases would require very high nickel oxidation states and defective phases such as hypothetical "Sr_2NiO_3" are unstable with respect to $SrNiO_{2+\delta}$ and SrO. However, stoichiometric solid solutions having acceptable tolerance factors and nickel oxidation states (e.g., $YSrNi^{III}O_4$ has calculated $t = 0.935$) could be envisaged. In fact, we find that only the stoichiometry $Y_{0.33}Sr_{1.67}Ni^{III}O_{3.67}$ is stable in this

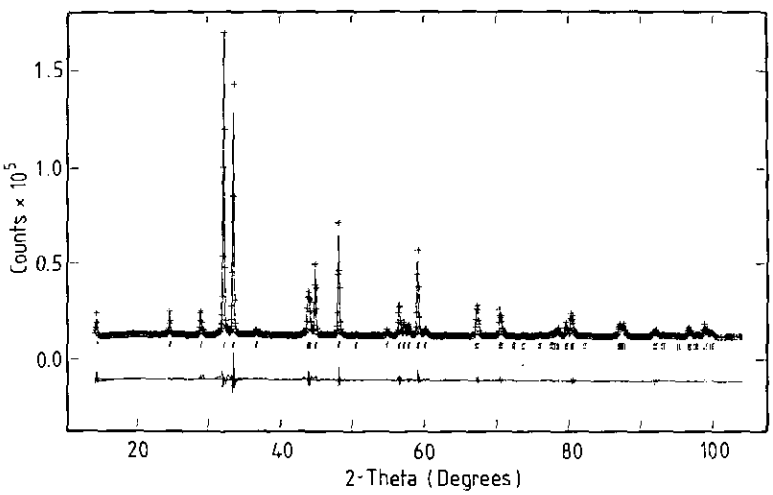

FIG. 2. Observed (crosses), calculated (full line), and difference profiles of $YSr_5Ni_3O_{11}$, showing position markers for reflections.

TABLE III

INTERATOMIC DISTANCES FOR $YSr_5Ni_3O_{11}$ (Å), WITH ESD'S IN PARENTHESES

Ni–O(1)	×3⅓	1.888 (1)
Ni–O(2)	×2	1.994 (6)
Mean		1.928 (4)
Y/Sr–O(1)	×3⅓	2.574 (1)
Y/Sr–O(2)	×1	2.407 (7)
Y/Sr–O(2)	×4	2.681 (1)
Mean		2.605 (3)

system at O_2 pressure 1 bar. The stability and localized electron behavior of this unusual $YSr_5Ni_3O_{11}$ composition can be rationalized through the refined crystal structure, as described below.

The structure refinement results in Table II and Fig. 2 show that $YSr_5Ni_3O_{11}$ has a tetragonal anion-defective K_2NiF_4 structure. Although X-ray diffraction is insensitive to potential Y/Sr order, the resultant ordering of oxygen displacements or vacancies might result in a detectable supercell. However, we find no evidence for any structural distortion or supercell, although electron microscopy and neutron diffraction will be used to investigate further these possibilities. Refinement of the oxygen occupation factors clearly demonstrates that the $\frac{1}{12}$ oxygen vacancies are present in the nickel oxide plane (O(1)) sites, and the refined oxygen content of 11.0(1) is in excellent agreement with the TGA results. These vacancies reduce the average Sr/Y and Ni coordination numbers from 9 and 6 to $8\frac{1}{3}$ and $5\frac{1}{3}$, respectively. The formation of vacancies in the $z = 0$ planes of anion deficient K_2NiF_4 type structures has been reported in other systems, for example $La_2LiO_{3.5}$ (*20*). The mean metal to oxygen distances for Sr/Y = 2.605 and Ni = 1.928 Å are close to those calculated from Shannon's radii for $(\frac{5}{6}Sr^{2+} + \frac{1}{6}Y^{3+})$ = 2.64 Å and low spin Ni^{3+} = 1.96 Å.

$YSr_5Ni_3O_{11}$ is unusual in having Y^{3+} and Sr^{2+} disordered over the same lattice sites despite the 20% disparity in their ionic radii of 1.075 and 1.31 Å, respectively. In the majority of yttrium strontium oxides the cations are ordered, with Sr^{2+} in a larger, more highly coordinated site. Local adjustments of the *A* cation sites may take place to accommodate the different cations, and this may explain the exact stoichiometry of this apparent solid solution. If we imagine $YSr_5Ni_3O_{11}$ as resulting from the substitution of Y^{3+} for Sr^{2+} in hypothetical "Sr_2NiO_4," with the formation of one oxygen vacancy adjacent to each Y^{3+} in order to reduce the size of the coordination sphere, then compositions $Y_ySr_{2-y}NiO_{4-y}$ result. The value of y is controlled by the nickel oxidation state $(=4 - 3y)$ in order to maintain charge balance. The highest nickel oxidation state attainable under 1 bar O_2 is 3+, giving the observed value of $y = \frac{1}{3}$.

The association of one oxygen vacancy

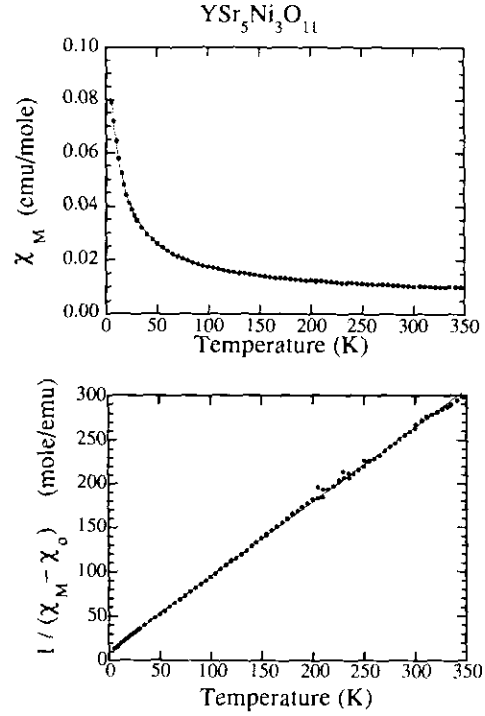

FIG. 3. Magnetic susceptibility (χ_M) and inverse of the corrected susceptibility ($1/(\chi_M - \chi_0)$) versus temperature for $YSr_5Ni_3O_{11}$. Closed circles represent experimental points, while the unbroken lines are given by the model in the text.

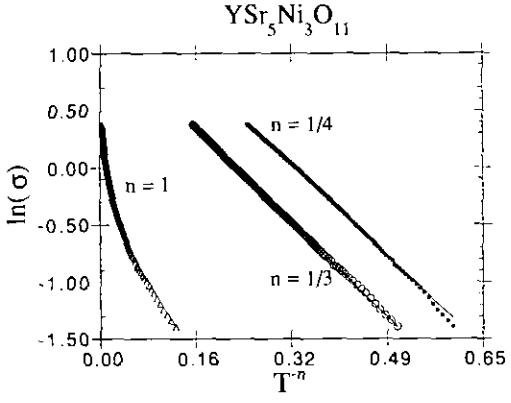

FIG. 4. ln(conductivity) versus T^{-n} (K^{-n}) for $YSr_5Ni_3O_{11}$ for $n = 1$, $\frac{1}{3}$, and $\frac{1}{4}$. Linear fits to the latter two plots are shown.

per Y^{3+} reduces the average Y^{3+} coordination number to ~7.5, whereas that for Sr^{2+} is ~8.5; this difference partly alleviates the size discrepancy between the cations. X-ray diffraction is not sensitive to this proposed local ordering and EXAFS will be used to investigate the Y and Sr environments. This model implies that the $RSr_5Ni_3O_{11}$ structure is only formed for R^{3+} cations significantly smaller than Sr^{2+} and so it is not observed in the R = La (*7*) and Nd (*10*) systems. Investigation of $RSr_5Ni_3O_{11}$ phases with smaller lanthanide cations is underway.

The vacancies on $\frac{1}{6}$ of the O(1) sites in the nickel oxide planes result in semiconducting behavior in $YSr_5Ni_3O_{11}$, unlike the related $RSrNiO_4$ phases (R = La, Nd) (*7–10*), which are metallic. The good fit of Mott's two-dimensional variable range hopping model to the data between 7 and 300 K is consistent with the high concentration of anion vacancies in the nickel oxide planes of this layered material. Variable range hopping behavior is also found in other transition metal oxides such as Fe_3O_4 and VO_2 (*21*) below the temperature at which a structural change accompanies a metal–insulator transition.

Magnetic susceptibility measurements of $YSr_5Ni_3O_{11}$ reveal Curie–Weiss behavior characteristic of low spin Ni^{3+} ($S = \frac{1}{2}$) down to 5 K and the observed μ_{eff} of 1.76(1) is very close to the spin-only moment (1.73). The oxygen vacancies frustrate the Ni–O–Ni magnetic interactions so that no deviations from the Curie–Weiss law are found down to 5 K, although the fitted $\Theta = -10.8$ K suggests that antiferromagnetic exchange occurs. The temperature independent Van Vleck contribution to the susceptibility of $\chi_0 = 0.0023(1)$emu/mole Ni^{3+} is comparable to those reported by Byeon and Demazeau (*22*) for several $A_2B_{0.5}Ni^{III}{}_{0.5}O_4$ compounds adopting the K_2NiF_4 structure.

Acknowledgments

The authors thank Dr. T. Rayment, Dr. J. D. Johnston, Mr. A. Carrington, Dr. J. R. Cooper, Mr. A. R. Jones, and Mr. A. J. Pauza for their assistance and discussions. M. J. is supported by the University of Sydney; Newman College, Melbourne University; and the Sir Robert Menzies Centre for Australian Studies, London.

References

1. J. M. BASSAT, P. ODIER, AND F. GERVAIS, *Phys. Rev. B* **35,** 7126 (1987).
2. D. J. BUTTERY, J. M. HONIG, AND C. N. R. RAO, *J. Solid State Chem.* **64,** 287 (1986).
3. C. N. R. RAO, D. J. BUTTERY, N. OTSUKA, P. GANGULY, H. R. HARRISON, C. J. SANDBERG, AND J. M. HONIG, *J. Solid State Chem.* **51,** 266 (1984).
4. D. J. BUTTERY AND J. M. HONIG, *J. Solid State Chem.* **72,** 38 (1988).
5. J. G. BENDORZ AND K. A. MÜLLER, *Z. Phys. B* **64,** 189 (1986).
6. J. GOPALAKRISHNAN, G. COLSMANN, AND B. REUTER, *J. Solid State Chem.* **22,** 145 (1977).
7. Y. TAKEDA, R. KANNO, M. SAKANO, O. YAMAMOTO, M. TAKANO, Y. BANDO, H. AKINAGA, K. TAKITA, AND J. B. GOODENOUGH, *Mater. Res. Bull.* **25,** 293 (1990).
8. K. SREEDHAR AND C. N. RAO, *Mater. Res. Bull.* **25,** 1235 (1990).
9. B. W. ARBUCKLE, K. V. RAMANUJACHARY, Z. ZHANG, AND M. GREENBLATT, *J. Solid State Chem.* **88,** 278 (1990).
10. Y. TAKEDA, M. NISHIJIMA, N. IMANISHI, R. KANNO, O. YAMAMOTO, AND M. TAKANO, *J. Solid State Chem.* **96,** 72 (1992).
11. J. SPALEK, Z. KAKOL, AND J. M. HONIG, *Solid State Commun.* **71,** No. 6, 511 (1989).
12. Z. KAKOL, J. SPALEK, AND J. M. HONIG, *J. Solid State Chem.* **79,** 288 (1989).

13. A. K. GANGULI, R. NAGARAJAN, G. R. RAO, N. Y. VASANTHACHARYA, AND C. N. RAO, *Solid State Commun.* **72,** No. 2, 195 (1989).
14. K. S. NANJUNDASWAMY, A. LEWICKI, Z. KAKOL, P. GOPALAN, P. METCALF, J. M. HONIG, C. N. R. RAO, AND J. SPALEK, *Physica C* **166,** 361 (1990).
15. H. M. RIETVELD, *J. Appl. Crystallogr.* **2,** 65 (1969).
16. A. C. LARSON AND R. B. VON DREELE, Los Alamos National Laboratory Report No. LA-UR-86-748 (1987).
17. N. F. MOTT, *Philos. Mag.* **19,** 835 (1969).
18. P. POIX, *J. Solid State Chem.* **31,** 95 (1980).
19. R. D. SHANNON, *Acta Crystallogr. Sect. A* **32,** 751 (1976).
20. J. P. ATTFIELD AND G. FÉREY, *J. Solid State Chem.* **80,** 112 (1989).
21. G. VON SCHULTESS AND P. WACHTER, *Solid State Commun.* **15,** 1645 (1974).
22. S-H. BYEON AND DEMAZEAU, *Mater. Lett.* **12,** 158 (1991).